Journal of Theoretical and Applied Information Technology
31st January 2015. Vol.71 No.3
© 2005 - 2015 JATIT & LLS. All rights reserved·
ISSN: 1992-8645 www.jatit.org E-ISSN: 1817-3195

RIVER BOUNDARY DELINEATION FROM REMOTELY SENSED IMAGERY BASED ON SVM AND RELAXATION LABELING OF WATER INDEX AND DSM

[1]PARAMATE HORKAEW, [2,3]SUPATTRA PUTTINAOVARAT, [3]KANIT KHAIMOOK

[1] School of Computer Engineering, Institute of Engineering, Suranaree University of Technology, Thailand
[2] Faculty of Science and Industrial Technology, Prince of Songkla University, Suratthani Campus, Thailand
[2, 3] School of Information Technology, Institute of Social Technology, Suranaree University of Technology, Nakhon Ratchasima, Thailand
E-mail: [1]phorkaew@sut.ac.th, [2]supattra.p@psu.ac.th, [3]kkanit@sut.ac.th

ABSTRACT

Topographic mapping of river boundary area is important in the environment management and hydrological modeling. In recent years, delineation of river by means of remotely sensed image classification has been widely investigated. Prime advantages of remote sensing technology for river delineation are reducing labor cost and time and elevating restrictions on ground surveys. However, these techniques are as yet to produce satisfactory result due to, for instance, the lack of an effective means of removing shadow and spurious noise. This paper proposes the boundary delineation of river from satellite image using Support Vector Machine (SVM) and two well accepted water indices (NDWI2 and MNDWI). In our framework, relaxation labeling was also incorporated in order to ensure reliable classification while suppressing spurious artifacts, inherited from the satellite imaging. The subsequent assessment suggested that MNDWI index yielded the most accurate classification and hence water extraction. The resolution of the delineated river braches was further enhanced by incorporating DSM data. The technique was then benchmarked against labor intensive manual tracing with promising consistency.

Keywords: *River Delineation, SVM, Relaxation Labeling*

1. INTRODUCTION

River delineation is one of primary steps toward hydrological modeling which in turn is important for environmental management. More specifically, reliable and accurate information on extent of water bodies is critical in a wide range of applications such as flood simulation, prediction and monitoring [1][2][3], watershed analysis [4] and change detection [5][6]. Delineation of river from remote sensing data as a consequent has widely been studied. It has also been extensively recognized that satellite image, aerial photography and SAR image are useful source of information for such procedure. The well accepted schemes found in literatures can be summarized as follow:

Separation between land and water in SAR images based on level set segmentation was applied successfully to river mapping extraction in real SAR images [7][8][9]. In their work, self-adaptive threshold Canny algorithm based on the maximum variance ratio was adopted to extract image edge. Edge based river extraction based on more robust and accurate algorithm than conventional Canny method was also proposed [10]. Waterway detection from satellite images by using curvelet transform and gradient vector flow (GVF) was studied, where the results were compared against wavelet based and Canny methods. Their results showed that the curvelet transform and GVF are superior to other methods [11], in terms of effectiveness and accuracy. A hill climbing algorithm combined with k-means clustering performed well on extracting the water areas from satellite image [12]. Gabor wavelet was used to enhance river texture and to remove noise from remotely sensed imagery. It could not detect however branches of the river [13]. A decision tree approach yields higher accuracy for identifying specific water areas compared to the conventional SVM approach. The results from [14] also suggest that the proposed approach using aerial imagery of R, G, B and NIR bands is a feasible and effective tool for measuring water areas. It was shown in [15] that Otsu method is more suitable for water body extraction from aerial imagery than the Mean Shift counterpart because the later may confuse the water bodies with vegetation. Focusing more onto

Journal of Theoretical and Applied Information Technology
31st January 2015. Vol.71 No.3
© 2005 - 2015 JATIT & LLS. All rights reserved
ISSN: 1992-8645 www.jatit.org E-ISSN: 1817-3195

image bands, [16] suggested that CIELAB color space and chromatic and textural analysis, combined with ISODATA classification, can extract water areas from RGB aerophotograph effectively and with relatively high generality. Shannon entropy was shown to be able to automatically segment water from land in aerial images. This method however does suffer from a limitation that it is unable to distinguish between smooth river water and areas of mowed fields, standing water or built environments which have similar textural characteristics [17].

It can be concluded from the above review that, image processing techniques have been widely adopted in river delineation from satellite images. They can be divided into two categories, i.e. single band and multi band [18][19]. One disadvantage of single bands method was that it is quite difficult to or is incapable of delineating river, when its pixels are mixed with different land cover types. Multi-bands method on the other hand, exploits advantage of reflective different of each band for classification between water and others. Multi band method for instance, NDWI, NDWI2, MNDWI, NDPI [5][20] [21][22] etc., has been showed to be more accurate that their single band counterparts.

Nonetheless, common shortcomings shared by the above methods, is the lack of an effective means of removing shadow and spurious noise. Moreover, pixels in narrower river may generate unstable spectral characteristics, which are difficult to be extracted. Therefore, this paper investigates the boundary delineation of river from satellite image using Support Vector Machine (SVM) and two of well acknowledged water indices (NDWI2 and MNDWI). In this work, relaxation labeling was incorporated in order to ensure accurate and reliable classification while suppressing spurious artifacts, inherited from the imaging modality. To improve the resolution further, the term extracted from DSM was also included.

2. THEORY AND RELATED MATERIALS

This section discusses material related to water area classification that has been previously adopted in the literatures, namely SVM, NDWI2, and MNDWI. Their applications as well as pros and cons are also addressed. Relaxation for connected component labeling by using these attributes is subsequently described.

2.1 Support Vector Machines: SVM

SVM is a supervised learning algorithm [23][24]. The prime advantage of the SVM over other conventional methods is that, it does not need to hold the normal distribution assumption in the input data and performs better even if only a small number of training samples are available. There are two types of SVMs, Linear and Non-linear SVM, which separates the data points using, respectively a linear and non-linear decision boundary. Linear SVM performs well on datasets that can be easily separated by a hyper-plane into two parts. But in some other cases where datasets are complex and thus difficult to classify using a linear kernel, Non-linear SVM classifiers are preferred. The rationale behind non-linear SVM classifier is to transform the dataset into a higher dimensional space where the data can be separated using a linear decision boundary. Let the training data consists of n vectors $\{(x_i, y_i), i = 1, 2,... n\}$. A class value or target $y_i \in (-1, 1)$ is associated to each vector, where n is the number of training samples. Linear classification is given as follows:

$$f_{w,b} = \operatorname{sgn}(\mathbf{w} \cdot \mathbf{x} + b) \quad (1)$$

where, **w** and **x** are vectors and the direction of w is perpendicular to the linear decision boundary. The vector **w** is determined using the training dataset. The separating hyperplane which maximizes the distance between the classes can be achieved by the following expression:

$$\min_{w,b} \frac{1}{2}\|w\|^2 \quad (2)$$

For nonlinear classes, a positive real value "slack variable" ξ_i should be introduced to relax the optimal hyperplane on the same side of the training class, so as to reflect the quantity proportional to the number of classification errors in the process of maximizing the margin of hyperplane. This tradeoff between the margin and misclassification is now controlled by a positive constant C such that:

$$\min_{w,b,\xi_i..\xi_k} \left[\frac{1}{2}\|w\|^2 + C\sum_{i=1}^{k} \xi_i \right] \quad (3)$$

The data vector **x** is usually mapped onto a higher dimensional Euclidean space through a non-linear vector Φ, by using a kernel function K in the design of a non-linear SVM. A kernel function is defined as $K = \Phi(\mathbf{x}_i) \cdot \Phi(\mathbf{x}_j)$. Subsequently, the non-linear classification function is given as follows:

$$f(x) = \operatorname{sgn}\left[\sum_{i=1}^{N} \alpha_i y_i K(\mathbf{x}_i \cdot \mathbf{x}_j) + b \right] \quad (4)$$

Where sgn is the sign function, K is the kernel function and the magnitude of α_i is determined by

© 2005 - 2015 JATIT & LLS. All rights reserved
ISSN: 1992-8645 www.jatit.org E-ISSN: 1817-3195

the parameter C, "." is dot product between the two vectors, b is the bias value. SVM requires a kernel function for mapping from the original space to feature space. The most frequently-used one are:

a) Polynomial kernel function, defined as:

$$K(\mathbf{x}_i \cdot \mathbf{x}_j) = (\gamma \mathbf{x}_i \cdot \mathbf{x}_j + b)^d \quad (5)$$

b) Radial basis function kernel function, defined as:

$$K(\mathbf{x}_i \cdot \mathbf{x}_j) = \exp\left(-\beta\gamma \left\|\mathbf{x}_i - \mathbf{x}_j\right\|^2\right) \quad (6)$$

c) Sigmoid kernel function, defined as:

$$K(\mathbf{x}_i \cdot \mathbf{x}_j) = \tanh(\gamma \mathbf{x}_i \cdot \mathbf{x}_j) \quad (7)$$

where γ is the gamma term in the kernel function for all kernel type, d is the polynomial degree term in the kernel function for the polynomial kernel, b is the bias term in the kernel function.

Opting suitable kernel function and model parameters has strong influence on the performance of classification. A number of publications on the classification based on remotely sensed imagery showed that RBF kernel function performs better in classification accuracy and classification time than other kinds of kernel function [6][25][26][27]. The success examples include land cover classification, road extraction, building extraction and land and water discrimination[28][29][30][31]. Accordingly, the RBF kernel function is hereby employed for the classification from Landsat images.

2.2 Normalized Difference Water Index: NDWI

NDWI2 was proposed by Mcfeeer [32]. Its expression is given as follows:

$$NDWI2 = \frac{Green - NIR}{Green + NIR} \quad (8)$$

where Green is the green band such as Landsat 5 band 2 and NIR is a near infrared band.

NDWI2 is widely applied especially for extracting water surface. In [5], surface changes of Lake Urmia, Iran during the period of 2000 – 2012 were analyzed. River or lake classification is also an area of interest in many literatures [18][33][34] [35][36][37]. Its value is nonetheless undermined by its inability to remove noise and shadow which are commonly found in satellite imaging modality. The values of NDWI2 fall within the interval between –1 and 1, ranging from low to high water content respectively.

2.3 Modified NDWI: MNDWI

MNDWI has made an improvement over the NDWI2 so that it is able to better distinguish water bodies from noise and built ups [21]. Its expression is given below:

$$MNDWI = \frac{Green - MIR}{Green + MIR} \quad (9)$$

where Green is the green band and MIR is a middle infrared band, similar to NDWI2. Thanks to this amendment, its applications are targeted closer to more habitant areas. It was, for instances, adopted in flood water mapping during the flood [38]. River and lake classification results were also improved [18][33][34][35][36][37]. Nonetheless, shadow and noise were not completely eliminated.

2.4 Digital Surface Model: DSM

DSM represents height information of the earth surface taken into account the objects such as, buildings, trees, etc. DSM is particularly applied in building extraction [39][40][41]. In addition, DSM is usually used for hydrological analysis, such as inundated area delineation [42], estimation of water surface elevation on inundated area [43], water area classification using Radarsat-1 SAR Imagery [44].

2.5 Relaxation Labeling

It is worth noting that classifications based on water indices classifies each pixel individually, discarding its surrounding contextual information. Isolated water or non-water pixels hence are often unfavorably interpreted on the contrary. Likewise, gradual variation of tonal intensity in the shadow area may also be misclassified.

An intermediate method called relaxation labeling overcomes this drawback by reclassifying object value using its neighborhood information. The objective of relaxation labeling is to minimize uncertainty and to improve consistency in assigning a label to each object in a group of related objects. Relaxation labeling was originally proposed by Rosenfield [45] and later modified and applied by many researcher in various fields [46][47][48][49].

With this technique, an initial probability of each object being assigned to a label is given and then gradually updated during subsequent iterative process. The probability is adaptively updated by reciprocal relation between contextual information:

$$q_i^k(\lambda) = \sum_j \sum_{\lambda'} r_{ij}(\lambda, \lambda')\ p_i^k(\lambda') \quad (10)$$

Journal of Theoretical and Applied Information Technology
31st January 2015. Vol.71 No.3
© 2005 - 2015 JATIT & LLS. All rights reserved
ISSN: 1992-8645 www.jatit.org E-ISSN: 1817-3195

$$p_i^{k+1}(\lambda) = \frac{p_i^k(\lambda)[1+q_i^k(\lambda)]}{\sum_{\lambda'} p_i^k(\lambda')[1+q_i^k(\lambda')]} \qquad (11)$$

Where $p_i^k(\lambda)$ is the probability of pixel i to belong class λ in the k iteration, $q_i^k(\lambda)$ is the total neighbor support r_{ij} (λ, λ') is the compatibility of pixel i belonging class λ with pixel j belonging class λ'.

2.6 Connected Component Labeling

Connected Component Labeling is simple method for grouping adjacent pixels sharing the same attributes [50], so as to identify homogeneous region for higher level analysis. This method has been entailed in several computer vision schemes (e.g., object segmentation and detection), normally after prerequisite classification [51][52][53].

3. METHODOLOGY

As discussed earlier that classification of water index using individual pixel is incapable of suppressing the noise resulted from built-up land or shadow. The aim of this paper is hence to further improve the traditional water body extraction from remote sensing (Landsat satellite images) based on the non-linear followed by adaptive classifications, (SVM and relaxation labeling). In our experiment, well accepted water indices, namely, NDWI2 and MNDWI were combined as a probability measure, whose resultant classifications were then compared.

3.1 Data Preparation

In this study, the remote sensing data, i.e., Landsat 5 and 8 images provided by USGS website were obtained as the inputs, while the ground truth segmentation was collected from manual digitizing. As an example to demonstrate the potential of our scheme, the study areas in Pathumthani Province (Chaopraya river basin) were considered. Figure 1 depicts respective Landsat 5 and 8 imageries of the areas and Table *I* lists Landsat 5 and 8 bands' characteristics (band assignment and corresponding wavelength). Each image has the dimension of 400 by 400 pixels and the resolution of 5 meters.

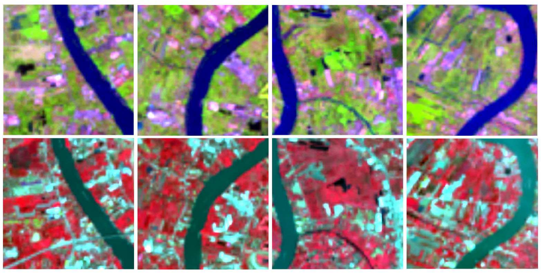

Figure 1: Selected examples of Landsat 5 and 8 images

Table 1: Comparisons among Landsat 5 and Landsat 8

Landsat 5 Bands (µm)		Landsat 8 Bands (µm)	
		Coastal/Aerosol (0.435-0.451)	Band 1
Band 1	Blue (0.45-0.52)	Blue (0.452-0.512)	Band 2
Band 2	Green (0.52-0.60)	Green (0.533-0.590)	Band 3
Band 3	Red (0.63-0.69)	Red (0.636-0.679)	Band 4
Band 4	NIR (0.760-0.90)	NIR (0.851-0.879)	Band 5
Band 5	SWIR (1.55-1.75)	SWIR-1(1.566-1.651)	Band 6
Band 6	TIR (10.40-12.50)	TIR-1 (10.60-11.19)	Band 10
		TIR-2 (11.50-12.51)	Band 11
Band 7	SWIR (2.08-2.35)	SWIR-2 (2.107-2.294)	Band 7
		Pan (0.503-0.676)	Band 8
		Cirrus (1.363-1.384)	Band 9

3.2 Water Index Classification

In our experiment, NDWI2 and MNDWI indices were calculated from Landsat 5 and Landsat 8, according to Table I. The classification of these indices traditionally required empirical thresholds whose values varied depending on land coverage components. Appropriately choosing the thresholds requires intervention from an expert as it needed to be able to discriminate between water, non-water, and mixture features. Moreover, determining these values by different experts gave differing decisions with high inter and intra observer variability. By employing SVM followed by relaxation labeling, no hard decision on the values are required, rather it iteratively assigns classes' probabilities based on non-linear discriminator and contextual gathering.

3.3 SVM Classification

Water region detection was achieved by applying a non-linear classifier on each pixel based on its water indices. In this work, only two classes, which are river and non-river, were considered. The training and testing data were randomly drawn from 8 satellite images (Landsat 5 and 8), with uniform distribution. For the training set, out of 600 random points, 297 points were of the river class while the remaining 303 were drawn from non-river class.

Journal of Theoretical and Applied Information Technology
31st January 2015. Vol.71 No.3
© 2005 - 2015 JATIT & LLS. All rights reserved.
ISSN: 1992-8645 www.jatit.org E-ISSN: 1817-3195

The testing set consisted of 200 points, 28 and 172 of which were respectively of river and non-river classes.

The SVM was trained using the pixel and the known classes of the training data. Input given to the SVM was varied by varying the number of features selected in the training dataset and also by RBF kernel function used by SVM. After training, independent testing dataset was classified. In order to assess the accuracy of the classifier, the distance from the testing samples to the separating plane was evaluated. The distance of misclassified test samples was compared with the margin value to determine whether they lied in the danger zone. Figure 2 and 3 present an example of non-linear separation using the SVM from training and testing datasets respectively. The yellow circles in Figure 2 and 3 are patterns belonging to class 1 (river area) and the black plus symbols are from class 2 (non-river area). The resultant SVM provided non-linear separation, indicated by the blue solid non-linear decision boundary.

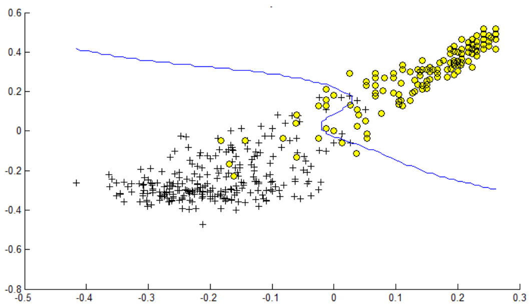

Figure 2: Decision boundary obtained from the training

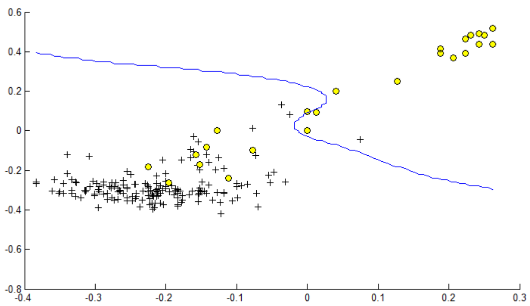

Figure 3: Decision boundary computed from the testing

3.4 Relaxation Labeling Process

Prior to iterative labeling, the process did require the initial probability values given to each pixel. In this context, a probability with Gaussian density function, whose random variable obtained from SVM, is adopted as it most resemblances the relationship between river and its indices. Although the Landsat 5 and 8 images have attractive qualities in terms of extracting water region, their main limitations are due to moderate-resolution (only 30 meter). Landsat data alone was hence incapable of extracting the narrow water bodies (as shown in Figure 3). Reasonable solution was therefore to add another probability argument term derived from the DSM image, as follow:

$$P(i) = \frac{1}{2}\left[\frac{1}{\sigma\sqrt{2\pi}} e^{\frac{-(x-\mu)^2}{2\sigma^2}} + (1 - DSM_i)\right] \quad (12)$$

where P(i) is the initial probability of the ith pixel, whose water index and Digital Surface Model value was given by x_i and DSM_i, respectively. μ is the mean, σ is its standard deviation.

As the iterations progressed, probabilities of those labels (a false positive – being river) which were opposed by neighbors (contextual support, not being river) became weaker, and vice versa. The updating of each pixel label accordingly proceeded such that the label assigned to river (or not-river) is consistent with label found within its neighborhood. This had preferred effect on removing spurious features as well as being robust against gradual cast shadow. The updating process was repeated until convergence, whereby the label supported most strongly by its neighbors will be assigned to that pixel. In our experiment, the sufficient number of iterations was set to the maximum of 20.

3.5 Connected Component Process

Groups of river pixels classified from the previous step served as an input to the connected component labeling. In this paper, 8-connectivity was chosen. Component having fewer pixel counts than a prescribed threshold (depending on the size of water body of interest) were rejected as well as those classified as non-river. The resulting image finally contained only delineated river.

4. RESULTS

Overall performance of river delineation was first assessed by visual inspection on water index of the original multiband images depicted in Figure 1. In Figure 4, (Landsat 5), and Figure 5, (Landsat 8), no noted difference between NDWI2 and MNDWI are present. Comparative delineation results corresponding to the Landsat images using 4 conventional methods (threshold on single water index) are illustrated in Figure 6 and 7, where false positive and negative are found in many locations. SVM classification based on water indices from Landsat 5 and 8 are displayed in Figure 8 and 9, where scattering misclassified pixels as river can be noticed. After applying relaxation labeling on the

Journal of Theoretical and Applied Information Technology
31st January 2015. Vol.71 No.3
© 2005 - 2015 JATIT & LLS. All rights reserved·
ISSN: 1992-8645 www.jatit.org E-ISSN: 1817-3195

SVM results are shown in Figure 10 and 11. As expected, although the spurious noise was remove successfully while being robust against gradually cast shadow, it failed to delineate narrower river branches Incorporating both SVM and DSM into the initial probability of relaxation labeling, yielded more satisfactory results as illustrated in Figure 12 and 13.

Concentrating closer has revealed further details. Comparing Figure 6 and 7 indicate that the conventional methods gave less accurate river delineation when using Landsat 8, compared with when using Landsat 5. On the other hand, Figure 8 and 9 implied that SVM classification from Landsat 5 performed worse than did so from the Landsat 8. Figure 12 and 13 indicated that our method resulted in most accurate of river and its branch delineation regardless of either of Landsat images used. Considering all of the methods studied, NDWI2 and MNDWI indices served equally well for both types of Landsat images.

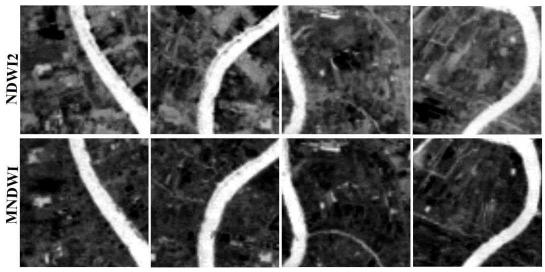

Figure 4: NDWI2 and MNDWI from Landsat 5

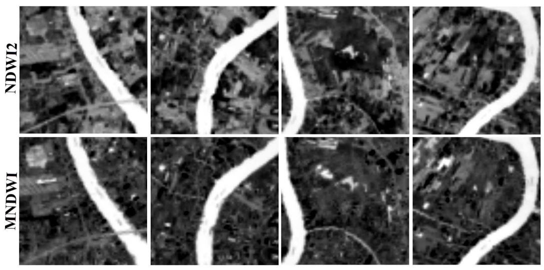

Figure 5: NDWI2 and MNDWI from Landsat 8

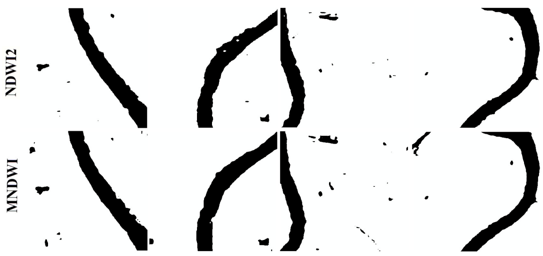

Figure 6: Original Method from Landsat 5

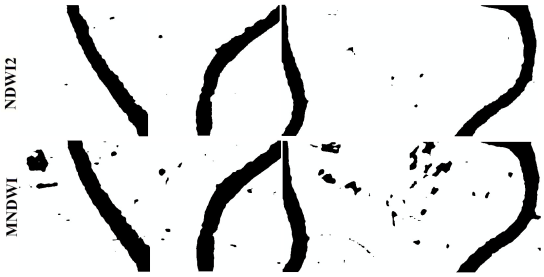

Figure 7: Original Method from Landsat 8

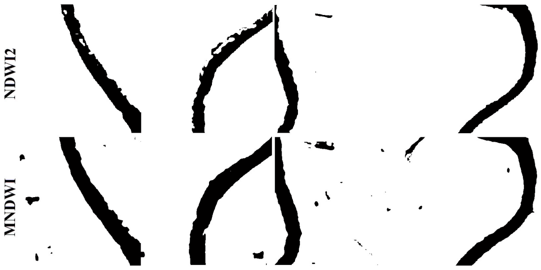

Figure 8: SVM Classification from Landsat 5

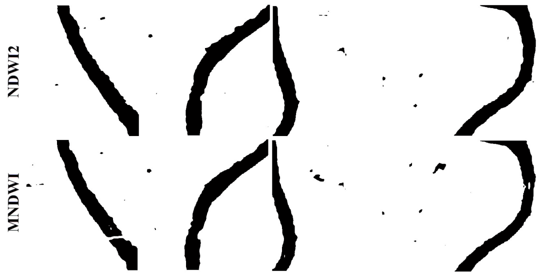

Figure 9: SVM Classification from Landsat 8

Figure 10: Relaxation Labeling Result of NDWI2 and MNDWI from Landsat 5

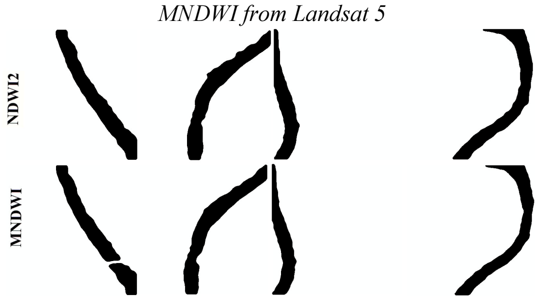

Figure 11: Relaxation Labeling Result of NDWI2 and MNDWI from Landsat 8

Journal of Theoretical and Applied Information Technology
31st January 2015. Vol.71 No.3
© 2005 - 2015 JATIT & LLS. All rights reserved.
ISSN: 1992-8645 www.jatit.org E-ISSN: 1817-3195

To quantitatively assess the suitability of river delineation using these techniques, they were compared against those digitized manually. To this end, accuracy and precision of using these indices were evaluated for Landsat 5 and Landsat 8 images, and are listed in TABLE 2 and 3, respectively.

Figure 12: Relaxation Labeling Result of NDWI2 and MNDWI from Landsat 5 and DSM

Figure 13: Relaxation Labeling Result of NDWI2 and MNDWI from Landsat 8 and DSM

The numerical results conform well to the above visual inspection. The comparison also suggests that when applicable, Landsat 5 should be preferred to Landsat 8, since it yield slightly better accuracy and precision for both NDWI2 and MNDWI.

Table 2: Accuracy assessment results of Landsat5

Water Index	Landsat 5 Satellite Images			
	Original Method	SVM	SVM +RRL +CCL	Purposed Method (SVM+RRL +CCL+DSM)
Image no.1				
NDWI2	97.15	96.43	96.49	98.97
MNDWI	97.19	97.26	97.84	98.97
Image no.2				
NDWI2	96.01	95.29	95.56	98.5
MNDWI	96.46	95.99	96.81	98.39
Image no.3				
NDWI2	96.16	93.55	93.66	97.39
MNDWI	95.93	96.43	96.53	97.36
Image no.4				
NDWI2	93.50	92.18	92.04	96.56
MNDWI	93.10	93.14	93.35	96.49
Average				
NDWI2	95.70	94.36	94.44	97.86
MNDWI	95.67	95.71	96.13	97.80

Table 3: Accuracy assessment results of Landsat8

Water Index	Landsat 8 Satellite Images			
	Original Method	SVM	SVM +RRL +CCL	Purposed Method (SVM+RRL +CCL+DSM)
Image no.1				
NDWI2	96.45	96.75	96.69	98.72
MNDWI	94.52	96.4	96.38	98.84
Image no.2				
NDWI2	93.57	95.56	95.61	98.15
MNDWI	93.27	95.03	95.28	98.24
Image no.3				
NDWI2	95.56	93.56	93.22	96.25
MNDWI	93.29	93.84	93.55	96.61
Image no.4				
NDWI2	90.63	90.65	90.28	95.33
MNDWI	87.72	90.08	90.15	95.75
Average				
NDWI2	94.05	94.13	93.95	97.11
MNDWI	92.20	93.84	93.84	97.36

5. CONCLUSIONS

SVM classification method has been found very promising for image processing applications. The method can produce comparable or even better results than conventional method for supervised classification. An excellent feature of SVM is that only small training set is needed to provide high performance results. However, for river delineation

© 2005 - 2015 JATIT & LLS. All rights reserved·
ISSN: 1992-8645 www.jatit.org E-ISSN: 1817-3195

SVM should be integrated with other techniques to improve accuracy.

This paper arrives at a conclusion that taking into account contextual information in water body classification and extraction yields more preferable results over the traditional water index based extraction, in terms of the robustness against both noise and shadow. Furthermore, by including DSM data, it can perform river delineation with at greater resolution, allowing the extraction narrower river branch. In our proposed framework, human expert intervention was minimally required.

The study was carried out in the hope that the proposed framework as well as corresponding experiment would serve as a guideline for applying higher level computer vision techniques combined with modern classification algorithm, in delineating of river. This information lays the foundation for other subsequent water based analysis such as flood simulation, in which the more accurate and the more reliable these primary data are prepared, the more preferable of the system in integration.

Future development directions also include water flow analysis based on extracted water body structure provided by our method for rainfall-runoff prediction and flood simulation. Conventionally, most flow direction analyses are based solely on the DEM and thus are inadequately realistic, compared to that when explicit river information is available. It is hence anticipated that river extracted with our proposed method will be generally more accurate and reliable than its counterparts obtained by using tedious stream-burning.

In order to enhance the proposed algorithm further, appropriate initial weights for probability estimation in equation (12) should be investigated. In addition, grayscale mathematical morphology may be considered and compared against relaxation labeling in terms of spurious noise reduction. To optimize the SVM learning, a range of its variations (kernels and training set preparation, etc.) that are known to be effective may be chosen to improve its performance and speed as well as spatial resolution.

REFRENCES:

[1] Puech, C., Hostache, R., Raclot, D., and Matgen, P., "Estimation of flood water levels by merging dem and satellite imagery using hydraulics laws through ai to enhances the estimates," *In Proceedings of Second Space for Hydrology Workshop ESA*, 2007, pp 17-24.

[2] Ahmed Shaker, Wai Yeung Yan, and Nagwa El-Ashmawy., "Panchromatic Satellite Image Classification for Flood Hazard Assessment," *Journal of Applied Research and Technology*, Vol. 10, pp. 902-911, 2012.

[3] Sudiana, D., and Rizkinia, M, "ALOS/ PALSAR Image Processing using DINSAR and LOG Ratio for Flood Early Detection in JAKARTA Based on Land Subsidence," *MAKARA of Technology Series*. Vol. 15, pp. 193-200, 2012.

[4] Xian, G., and Crane, M., "Assessments of urban growth in the Tampa Bay watershed using remote sensing data", *Remote Sensing of Environment*, Vol.97, No.2, 2005, pp.203-215.

[5] Rokni, K., Ahmad, A., Selamat, A., and Hazini, S., "Water Feature Extraction and Change Detection Using Multitemporal Landsat Imagery", *Remote Sensing*, Vol.6, No.5, 2014, pp.4173-4189.

[6] Kuo, B. C., Ho, H. H., Li, C. H., Hung, C. C., and Taur, J. S, "A Kernel-Based Feature Selection Method for SVM With RBF Kernel for Hyperspectral Image Classification", IEEE *Journal of Selected Topics in Applied Earth Observation and Remote Sensing*, Vol.7, No.10, 2014, pp. 317-326.

[7] Wang Xiaoliang and Li Chunsheng, "River boundaries extraction in mountain areas for SAR images with fusing GIS information", *In Radar (Radar), 2011 IEEE CIE International Conference,* Chengdu, China: IEEE, 2009, pp. 1586-1588.

[8] Silveira, M., and Heleno, S, "Water/land segmentation in SAR images using level sets", *In Image Processing, 2008. ICIP 2008. 15th IEEE International Conference*, San Diego, California, USA: IEEE, 2008, pp. 1896-1899.

[9] Margarida Silveira and Sandra Heleno, "Classification of Water Regions in SAR Images using Level Sets and Non-Parametric Density Estimation", *In IEEE International Conference on Image Processing ICIP 2009*. Cairo, Egypt: IEEE, 2009, pp. 1685-1688.

[10] Zhao, J., Yu, H., Gu, X., and Wang, S, "The edge detection of river model based on self adaptive Canny Algorithm and connected domain segmentation", *In Intelligent Control and Automation (WCICA), 2010 8th*, World Congress Jinan, China: IEEE, 2010, pp. 1333-1336.

[11] Xiao, Moyan, et al. "Edge detection of riverway in remote sensing images based on curvelet transform and GVF Snake", *Spatial Accuracy Assessment in Natural Resources and Environmental Sciences*, Shanghai, PR China, 2008, pp.334-351.

© 2005 - 2015 JATIT & LLS. All rights reserved·
ISSN: 1992-8645 www.jatit.org E-ISSN: 1817-3195

[12] Shah, M. V., Choudhary, M. A., and Tewari, K, "River extraction from satellite image", *International Journal of Computer Science*, Vol.8, No.4, 2011, pp. 386-391.

[13] Wang, K., Feng, X., Xiao, P., and Wu, G, "The research on recognition and extraction of river feature in IKNOS based on frequency domain", *In Sixth International Symposium on Multispectral Image Processing and Pattern Recognition*, Yichang, China, 2009, pp. 749533-749533.

[14] Xiao, G., and Tien, D, "An object-based classification approach for surface water detection", *International journal of intelligent systems technologies and applications*, Vol.9, No.3, 2010, pp. 218-227.

[15] Macedo-Cruzl, A., Pajares-Martinsanz, G., and Santos-Pefias, M, "Unsupervised classification of images in RGB color model and Cluster validation techniques", *In IPCV* 2010, pp. 526-532.

[16] Zhao, M., Shang, H., Huang, W., Zou, L., and Zhang, Y, "Water Area Extraction from RGB Aerophotograph Based on Chromatic and Textural Analysis", *In GEOProcessing 2011, The Third International Conference on Advanced Geographic Information Systems, Applications, and Services*, 2011, pp. 46-52.

[17] McKay, P., Blain, C. A., and Linzell, R, "Automated identification of rivers and shorelines in aerial imagery using image texture", *In SPIE Defense, Security, and Sensing International Society for Optics and Photonics*, 2011, pp. 80300G-80300G.

[18] Haibo, Y., Zongmin, W, Hongling, Z, and Yu, G., "Water body extraction methods study based on RS and GIS", *Procedia Environmental Sciences*, Vol.10, 2011, pp. 2619-2624.

[19] Li, M., Xu, L., and Tang, M, "An Extraction method for Water Body of Remote Sensing Image Based on Oscillatory Network", *Journal of Multimedia*, Vol.6, No.3, 2011, pp.252-260.

[20] Lacaux, J. P., Tourre, Y. M., Vignolles, C., Ndione, J. A., and Lafaye, M, "Classification of ponds from high-spatial resolution remote sensing: Application to Rift Valley Fever epidemics in Senegal", *Remote Sensing of Environment*, Vol. 106, No.1, 2007, pp. 66-74.

[21] Xu, H, "Modification of normalised difference water index (NDWI) to enhance open water features in remotely sensed imagery", International *Journal of Remote Sensing*, Vol.27, No.14, 2006, pp.3025-3033.

[22] Dambach, P., Machault, V., Lacaux, J. P., Vignolles, C., Sié, A., and Sauerborn, R, "Utilization of combined remote sensing techniques to detect environmental variables influencing malaria vector densities in rural West Africa", *Int J Health Geogr*, Vol.11, No.8, 2012, pp. 1-12.

[23] Cortes, C., and Vapnik, V, "Support-vector networks", *Machine learning*, Vol.20, No.3, 1995, pp. 273-297.

[24] Vapnik, V, "The support vector method of function estimation", *In Nonlinear Modeling*, Springer US, 1998, pp. 55-85.

[25] Ge, Q. Z., Ling, Z. C., Qiong, L., Hui, X. X., and Zhang, G, "High efficient classification on remote sensing images based on SVM", *Proc. of the International Archives of the Photogrammetry, Remote Sensing and Spatial Information Sciences*, 2008, pp. 1011-1014.

[26] Sakthi G., and Nedunchezhian, R., "Novel Optimization Technique for Classification of Remote Sensing Data using SVM", *Journal of Theoretical and Applied Information Technology*, Vol.59, No.3, 2014, pp. 725-734.

[27] Shahkooeei, E., Arekhi, S., and Kani, A. N, "Remote sensing and GIS for mapping and monitoring land cover and land use changes using support vector machine algorithm (Case study: Ilam dam watershed)", *International Research Journal of Applied and Basic Sciences*, Vol.8, No.4, 2014, pp. 464-473.

[28] Jin, H., Feng, Y., and Shen, Y, "Accurate urban road model reconstruction from high resolution remotely sensed imagery based on Support Vector Machine and Gabor filters", *In: Joint Urban Remote Sensing Event (JURSE)*, 11-13 April, Munich, Germany, Germany, 2011.

[29] Baluyan, H., Joshi, B., Al Hinai, A., and Woon, W. L, "Novel Approach for Rooftop Detection Using Support Vector Machine", *ISRN Machine Vision*, Vol.2013, 2013, pp. 1-11.

[30] Lv, W., Yu, Q., and Yu, W, "Water extraction in SAR images using GLCM and Support Vector Machine",*In Signal Processing 2010 IEEE 10th International Conference*, 2010, pp. 740-743.

[31] Klemenjak, S., Waske, B., Valero, S., and Chanussot, J, "Unsupervised river detection in RapidEye data", *In IGARSS*, 2012, pp. 6860-6863.

© 2005 - 2015 JATIT & LLS. All rights reserved·
ISSN: 1992-8645 www.jatit.org E-ISSN: 1817-3195

[32] MCFEETERS, S.K., "The use of normalized difference water index (NDWI) in the delineation of open water features", *International Journal of Remote Sensing*, Vol.17, No.7, 1996, pp.1425–1432.

[33] Wang, Y., Huang, F., and Wei, Y, "Water body extraction from LANDSAT ETM+ image using MNDWI and KT transformation", *In Geoinformatics 21st International Conference*, 2013, pp.1-5.

[34] Li, M., Xu, L., and Tang, M, "An Extraction method for Water Body of Remote Sensing Image Based on Oscillatory Network", *Journal of Multimedia*. Vol.6, No.3, 2011, pp.252-260.

[35] Chao, Z., and Sheng, M, "Study on extraction methods for water information in Nantong city, China using Landsat ETM+ data", In Remote Sensing, *Environment and Transportation Engineering (RSETE), 2011 International Conference*, 2011, pp. 771-774.

[36] Jiang, H., Feng, M., Zhu, Y., Lu, N., Huang, J., and Xiao, T. "An Automated Method for Extracting Rivers and Lakes from Landsat Imagery", *Remote Sensing*, Vol.6, No.6, 2014, pp.5067-5089.

[37] Shen, L., and Li, C, "Water body extraction from Landsat ETM+ imagery using adaboost algorithm", *In Geoinformatics, 18th International Conference*, 2010, pp.1-4.

[38] Baig, M. H. A., Zhang, L., Wang, S., Jiang, G., Lu, S., and Tong, Q., "Comparison of MNDWI and DFI for water mapping in flooding season", *In IGARSS*, 2013, pp. 2876-2879.

[39] Weidner, U, "Digital surface models for building extraction", *In Automatic extraction of man-made objects from aerial and space images (II) Birkhäuser Basel*, 1997, pp. 193-202.

[40] Brédif, M., Tournaire, O., Vallet, B., and Champion, N, "Extracting polygonal building footprints from digital surface models: A fully -automatic global optimization framework", *ISPRS Journal of Photogrammetry and Remote Sensing*, Vol.77, 2013, pp. 57-65.

[41] Li Y., Lin Z. L., and Shimamura H, "Integrated method of building extraction from Digital Surface Model and imagery", *The International Archives of the Photogrammetry, Remote Sensing and Spatial Information Sciences*, Vol. XXXVII. Part B3b, 2008, pp. 81–86.

[42] Leventi, I., Nalbantis, I., and Georgopoulos, A, "On the use of Digital Surface Models and hydrological/hydraulic models for inundated area delineation", *In Environment Hydraulics*, 2010, pp. 875-880.

[43] Yorozuya, A., Kamimera, H., Okazumi, T., Iwami, Y., and Kwak, Y, "Estimation of water surface elevation on inundated area using satellite based information",*In MODSIM2013, 20th International Congress on Modelling and Simulation*, Modelling and Simulation Society of Australia and New Zealand, 2013, pp. 2353-2359.

[44] Song, Y. S., Sohn, H. G., and Park, C. H, "Efficient water area classification using Radarsat-1 SAR imagery in a high relief mountainous environment", *Photogrammetric Engineering & Remote Sensing*, Vol.73, No.3, 2007, pp. 285-296.

[45] Rosenfeld, A., R. Hummel and S. Zucker, "Scene labelling using relaxation operations", *IEEE Transactions on Systems*, Man and Cybernetics, Vol.SMC-6, 1976, pp.420- 433.

[46] Eklundh, J. O., Yamamoto, H, and Rosenfeld, A., "A relaxation method for multispectral pixel classification", *Pattern Analysis and Machine Intelligence, IEEE Transactions*, Vol.1, 1980, pp.72-75.

[47] Rizvi, I., Mohan, B. K., and Narayana, E. L, "Accuracy Enhancement of Object Based Image Classification using Relaxation Labeling Process for High Resolution Satellite Image", *In ASPRS 2011 Annual Conference*, 2011, pp. 1-8

[48] Paclık, P., Duin, R. P., Van Kempen, G. M., and Kohlus, R., "Segmentation of multi-spectral images using the combined classifier approach", *Image and Vision Computing*, Vol.21, No.6, 2003, pp.473-482.

[49] Zhou, Q., and Sun, H, "Digital image classification using label relaxation for improved ground vegetation cover investigation", *In Procs. 8th Australasian Photogrammetry and Remote Sensing*, 1996, pp. 25-29.

[50] Suzuki, K., Horiba, I., and Sugie, N, "Linear-time connected-component labeling based on sequential local operations", *Computer Vision and Image Understanding*, Vol.89, No.1, 2003, pp.1-23.

[51] Yapa, R. D., and Harada, K., "Connected component labeling algorithms for gray-scale images and evaluation of performance using digital mammograms", *International Journal of Computer Science and Network Security*, Vol.8, No.6, 2008, pp.33-41.

© 2005 - 2015 JATIT & LLS. All rights reserved·
ISSN: 1992-8645 www.jatit.org E-ISSN: 1817-3195

[52] Jau, U. L., and Teh, C. S, "Real-time object-based video segmentation using colour segmentation and connected component labeling", *In Visual Informatics: Bridging Research and Practice*, Springer Berlin Heidelberg, 2009, pp. 110-121.

[53] Karthikeyan, V., Vijayalakshmi, V. J., and Jeyakumar, P, "License Plate Segmentation Using Connected Component Analysis", *Journal of Electronics and Communication Engineering*, Vol.4, No.5, 2013, pp.18-24.